REPORT No. 29

June, 1949

THE COLLEGE OF AERONAUTICS.

CRANFIELD

The Buckling in Compression of Panels with Square Top-Hat Section Stringers

-by-

W.S. Hemp, M.A., and K.H. Griffin, B.Sc..

of the Department of Aircraft Design.

--oOo--

SUMMARY

A simplified panel model is described, together with a number of assumptions about the mode of its buckling. The approach to the calculation of the buckling stress is by splitting the panel into a number of flat plates and treating these by the ordinary plate theory. Use of the boundary conditions between these plates leads to a relation between the buckling stress and the variables of the panel geometry.

The results thus obtained are compared with two sets of recent experimental work; and an appendix is included to show the effect of initial panel irregularities on the experimental determination of buckling stresses.

GWF

Table of Principal Symbols Used

L	=	Stringer height
b	=	Stringer pitch
t	=	Skin thickness
t_s	=	Stringer thickness
f_b	=	Buckling stress
f_o	=	$3.62Et^2/b^2$
f_a	=	Average stress in a skin panel
f_e	=	Edge stress in a skin panel
H	=	Amplitude of buckle
H_o	=	Amplitude of initial irregularity
λ	=	Wavelength of buckled form

Other subsidiary symbols are defined where they occur in the report.

PART I : THEORETICAL CONSIDERATIONS

1.1. Statement of the Problem

We investigate the local buckling of stringer-skin combinations with a cross-section perpendicular to the direction of the stringers as shown in Fig.1. The stringers are square, of side h, and are uniformly spaced to a pitch b. The skin and stringers have thicknesses t, t_s respectively.

Fig. 1.

Physical Assumptions:-

(1) The panels are large enough in both directions for edge-effects to be ignored.

(2) The stringers have square corners and no flanges, their sides being attached directly to the skin.

(3) The panels buckle under the action of a compressive stress f, parallel to the direction of the stringers.

(4) The buckling is sinusoidal in the direction of compression, of wavelength 2λ. By (1), λ may vary continuously, and its magnitude is determined by a minimum process (§ 1.2)

(5) Perpendicular to the direction of compression, the buckling is symmetrical with respect to each stringer, in a mode as shown in Fig. 2.

/(6) During ...

(6) During buckling, the stringer corners A,B, C,D (Fig.2) remain fixed in space, and the right angles at these corners are conserved.

(7) Deflections are small enough for the Principle of Superposition to hold.

Fig. 2.

1.2. Method of Treatment

We regard the panel shown in Fig. 1, as if it were built up of separate flat plates, each buckling under the action of the compressive stress f and moments distributed along the edges parallel to f. These moments are caused by interaction with the other plate(s) attached to this edge. Since the buckling is symmetrical about the stringers, the two stringer sides will have similar modes of buckling, and we need only consider one of them. One boundary condition, that of equilibrium, is that the sum of the moments at each junction should be zero. The other, arising from assumption (6), is that the angles of rotation at the edges of adjoining plates should be equal.
The four basic plates are shown in Fig. 3.

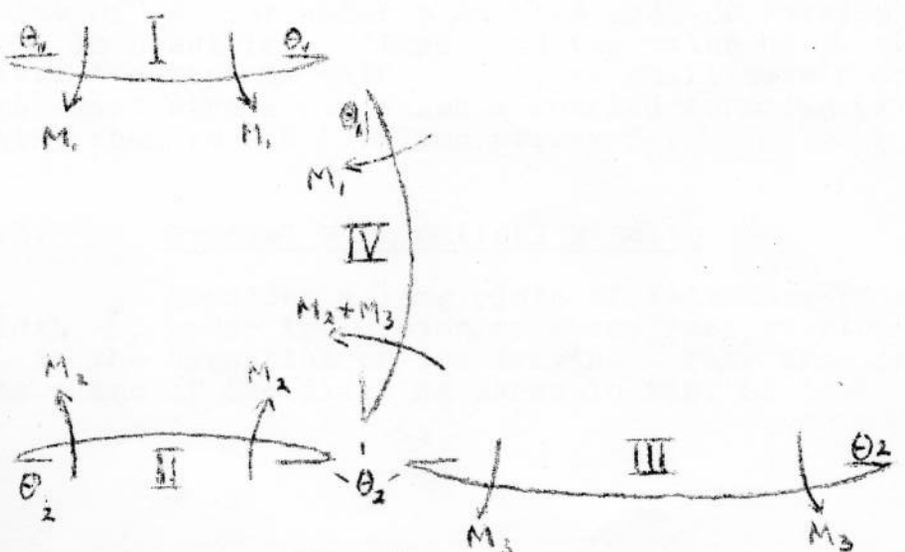

Fig. 3.

/Using ...

Using assumption (7), we may analyse the deflections of plate IV into

IVa: A symmetrical buckling, by moments $\frac{1}{2}(M_1 + M_2 + M_3)$ to edge angles $-\frac{1}{2}(\theta_1 + \theta_2)$

IVb: An antisymmetric buckling, by moments $\frac{1}{2}(M_2 + M_3 - M_1)$ to edge angles $\frac{1}{2}(\theta_1 - \theta_2)$

Thus we deal with the deflections of the five plates listed below.

Plate	Width	Thick-ness	Moments	Edge-Angle	Mode
I	h	t_s	M_1	θ_1	Symmetric
II	h	t	M_2	θ_2	"
III	b-h	t	M_3	θ_2	"
IVa	h	t_s	$\frac{1}{2}(M_1+M_2+M_3)$	$-\frac{1}{2}(\theta_1+\theta_2)$	"
IVb	h	t_s	$\frac{1}{2}(M_2+M_3-M_1)$	$\frac{1}{2}(\theta_1-\theta_2)$	Antisymmetric

Applying the formulae of plate theory to each of these five "basic plates", we obtain relations between the unknown moments and rotation-angles at each edge (§ 1.3). These relations contain the stress f and the half-wavelength λ. There are five of these relations, containing three independent moments and two independent angles. We may eliminate the moments and angles and obtain an equation between f and λ. This gives the value of f for which a buckled mode of wavelength 2λ is possible. If we find the value of λ which gives the minimum value of f, we shall have found the least stress for which a buckled form can exist. This, then, is the buckling stress f_b.

1.3. General Mathematical Results

Consider a long plate of thickness τ and width ℓ, under the action of a compressive stress f in the direction of its length. Take axes in the plane of the plate as shown in Fig. 4.

/Fig. 4. ...

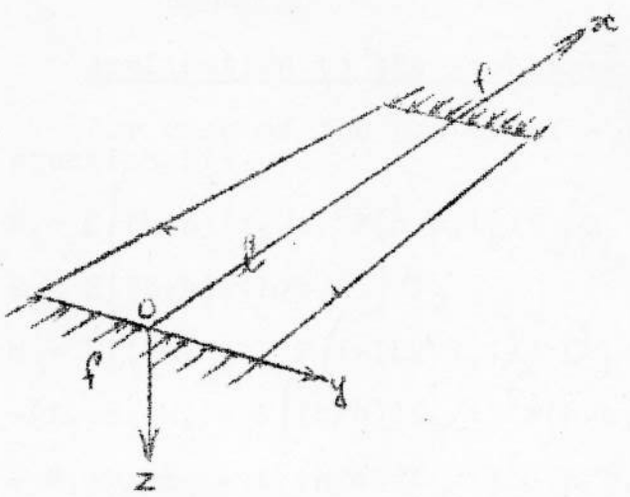

Fig. 4.

From assumption (4) the normal deflection must be of the form

$$W = W_o(y)\sin(\pi x/\lambda)$$

Since the deflections are proportional to $\sin(\pi x/\lambda)$, the rotation angles θ at $y = \pm \ell/2$ will vary likewise, as will the couples M acting on these edges.

Let $\theta = \theta_o \sin(\pi x/\lambda)$, $M = M_o \sin(\pi x/\lambda)$,

where θ_o, M_o are constants. Then it can be shown that for equilibrium under the action of f, we must have

$$M/\theta = M_o/\theta_o = \begin{cases} K(\ell/b)(\tau/t)^2 F_{f/f_o,\lambda/b}(\ell/b,\tau/t) & \text{(symmetric buckling)} \\ K(\ell/b)(\tau/t)^2 G_{f/f_o,\lambda/b}(\ell/b,\tau/t) & \text{(antisymmetric buckling)} \end{cases} \quad (1)$$

where

$$\left.\begin{aligned} F_{f/f_o,\lambda/b}(\ell/b,\tau/t) &= 1/\left[\left(\frac{\alpha\ell}{2}\right)\tanh\left(\frac{\alpha\ell}{2}\right)+\left(\frac{\beta\ell}{2}\right)\tan\left(\frac{\beta\ell}{2}\right)\right] \\ G_{f/f_o,\lambda/b}(\ell/b,\tau/t) &= 1/\left[\left(\frac{\alpha\ell}{2}\right)\coth\left(\frac{\alpha\ell}{2}\right)-\left(\frac{\beta\ell}{2}\right)\cot\left(\frac{\beta\ell}{2}\right)\right] \end{aligned}\right\} \quad (2)$$

and

$$\left.\begin{matrix} 1/\alpha \\ 1/\beta \end{matrix}\right\} = b\sqrt{\left[6.287(\pi b/\lambda)(t/\tau)\sqrt{(f/f_o)} \pm (\pi b/\lambda)^2\right]}\left[\begin{matrix} + \text{ for } \alpha \\ - \text{ for } \beta \end{matrix}\right];$$

K is a function of $f/f_o, \lambda/b$ only; and $f_o = 3.62E(t/b)^2$ is the buckling stress of a long plate of width b, thickness t, having simply supported edges.

/1.4. Application ...

1.4. Application to the Problem:-

For each of the plates I - IVb we write down equation (1):-

$$\left.\begin{aligned} \text{I} \quad & M_1 = K\left[(h/b)(t_s/t)^2 F(h/b, t_s/t)\right]\theta_1 \\ \text{II} \quad & M_2 = K\left[(h/b)F(h/b,1)\right]\theta_2 \\ \text{III} \quad & M_3 = K\left[(1-(h/b))\,F\left(1-(h/b),1\right)\right]\theta_2 \end{aligned}\right\} \qquad (3)$$

$$\left.\begin{aligned} \text{IVa} \quad & -(M_1+M_2+M_3) = K\left[(h/b)(t_s/t)^2 F(h/b, t_s/t)\right](\theta_1+\theta_2) \\ \text{IVb} \quad & -M_1+M_2+M_3 = K\left[(h/b)(t_s/t)^2 G(h/b, t_s/t)\right](\theta_1-\theta_2) \end{aligned}\right\} \qquad (4)$$

Substituting for M_1, M_2, M_3 from (3) in (4), and then eliminating θ_1, θ_2 and writing $h = b/n$; $F(r/n, \tau/t) = F_r^n(\tau/t)$, we obtain

$$\left.\begin{aligned} &\left(3F_1^n(t_s/t)+G_1^n(t_s/t)\right)\left(F_1^n(1)+(n-1)F_{n-1}^n(1)\right) \\ &\quad +(t_s/t)^2 F_1^n(t_s/t)\left(F_1^n(t_s/t)+3G_1^n(t_s/t)\right) = 0 \end{aligned}\right\} \qquad (5)$$

(5) is an implicit equation in the non-dimensional parameters $f/f_\sigma, \lambda/b, t_s/t, h/b(=1/n)$. Thus, given $t_s/t, h/b$ (the geometry of the panel), we can determine the ratio f_b/f_o as outlined in § 1.2.

1.5. Calculation of Results

For a given value of b/λ, the left-hand-side of (5) was tabulated at intervals for f/f_o of 0.1. The value of $f_b/f_\sigma(b/\lambda)$ was then obtained by graphical inverse interpolation to zero. This was done for several values of b/λ; f_b/f_σ was then plotted against b/λ, and its minimum value found graphically. The results of these calculations are shown in Table I.

Special Cases:-

(1) t_s/t large:- If $t \to 0$ while t_s remains finite, then the skin alone will buckle, the stringers exerting a clamping effect. So the buckling stress is that for clamped-edge plates of width (b-h), thickness t. $(h < b/2)$

$$\text{i.e.} \quad f_b = 6.31E\left(t/(b-h)\right)^2 \qquad (6)$$

$$f_b/f_o = 1.74/\left(1-(h/b)\right)^2$$

/(2) t_s/t small :- ...

(2) t_s/t small:- When t_s/t is small, (5) approximates to

$$\left(3F_1^n(t_s/t)+ G_1^n(t_s/t)\right)\left(F_1^n(1)+(n-1)F_{n-1}^n(1)\right) = 0 \quad (7)$$

Thus its solution is the smallest value of f/f_0 which makes either factor of the left-hand side of (7) vanish.

Now $$F_1^n(1)+(n-1)F_{n-1}^n(1) = 0 \quad (8)$$

is the buckling equation for the skin held at points alternately h,(b-h) apart. i.e. this is the case where the stringers exert no rotatory influence on the skin, but are merely stiff enough in their own plane to prevent normal displacement of the skin at their corners. Thus the buckling mode is as in Fig. 5.

Fig. 5.

As h/b increases, the stringers buckle first, and

$$3F_1^n(t_s/t) + G_1^n(t_s/t) = 0 \quad (9)$$

is the buckling equation for the stringers clamped by the unbuckled skin, as in Fig. 6.

Fig. 6.

(9) has the explicit solution

$$f_b/f_o = 1.17(t_s/t)^2/(h/b)^2 \quad (10)$$

where $b/\lambda = 1.125\ b/h$

/Thus ...

Thus for a given (small) t_s/t the solution of (5) is initially the curve which is the solution of (8), and after their intersection, by the cubical hyperbola whose equation is (10). Near the intersection, when both factors of the second term of (5) are small, the first term is no longer negligible compared with them, and its effect is to "round off the corner" of the intersection.

The final result of these calculations is shown in Fig.7.

1.6. Variations from Assumptions

It will be noted that up to the present no account has been taken of the fact that "practical" stringers have rounded corners. An attempt has been made to allow for this in the following manner.

The plates forming the stringers are unaltered, but the condition of conservation of angles is replaced. Using the theory of cylindrical shells, a change in angle at the corners is inserted, compatible with the bending of a cylindrical quadrant of the required radius and thickness under the given moments. This leads to new terms in the buckling equation (5), which is then solved as before.

This was done with a radius of h/10 for the cases $b/h = 5$, $t_s/t = 1, 1.33$ and also the case $t = 0$. In none of these was the drop in f_b/f_o greater than 3%. Also, it will be seen that this is necessarily an over-estimate of the actual effect, as there is assumed to be no reduction in the dimensions of the stringer plates. In fact, the rounding of the corners reduces the width of the stringer top and sides, increasing their stiffness , and partly counter-balancing the effect of the increased flexibility introduced.

It was, therefore, decided that the effect of the curved stringer corners could safely be neglected.

It is difficult to allow for the stringer flanges, as their effect will vary with the method of construction employed. It is clear, however, that the effect will be to increase the stiffness of panel III, thus increasing the buckling stress. However, for small $t_s/t, h/b$, the effect should only be small.

/PART II : ...

PART II : COMPARISON WITH EXPERIMENT

2.1. Work of A.J. Monk

In preparing his thesis for the Diploma of the College of Aeronautics, Lt.(E) A.J. Monk tested 36 panels of construction similar to that considered in Part I. These panels had four skin sections supported by five stringers, and were square, giving a ratio (panel length/stringer pitch) of approximately 4.

The stringers were of height 1", with $\frac{1}{2}$" flanges, and were riveted to the panels at a rivet pitch of $\frac{3}{4}$". The stringers were spaced to pitches of 3,4,5,6,7,8 inches giving values of h/b between 0.125 and 0.333. The ratio t_s/t covered the values 0.35, 0.45, 0.60, 0.75, 1.00, 1.33.

The ends of the panels were cast in a low melting-point alloy, and machined flat and parallel before testing. Two methods of estimating the buckling-stress were used. The first was to find the point where the load-strain curve changed direction. Secondly, the square of the buckle-amplitude was plotted against the strain. This should give a straight line intersecting the strain axis at the buckling-strain.

The results of these tests showed appreciable scatter, both between the two methods of estimation for the same panel, and between the various panels. In some of the estimations (mostly by the (amplitude)^2-strain method), no reliable answer could be obtained, as the curves bore little resemblance to the expected form. In less doubtful cases an estimate has been made, and a (?)appended to the entry in the diagram. These results, plotted against the appropriate theoretical curves, are shown in Fig. 8.

The scatter and the small number of panels tested make it difficult to obtain either confirmation or refutation of the theory, and indicate the need for a large-scale test programme with statistical analysis of the results. However, the experimental values show quite fair agreement with the theory.

/2.2. N.A.C.A. Test ...

2.2. N.A.C.A. Test Programme

Quite an extensive programme of panel testing was carried out by Messrs. W.A. Hickman and N.F. Dow at the Langley Memorial Laboratory during 1946-8 (Ref.1). These tests were carried out primarily to obtain failing-stress values, but buckling-stress measurements were also taken. These were done by the "strain-reversal" method. (Ref.2).

Panels were tested having four values of t_s/t, namely 0.39, 0.63, 1.00, 1.25. The stringer thickness in each case was 0.04". The stringer flange widths b_A were respectively 0.85", 0.75", 0.65", 0.55". For each value of t_s/t, h/t_s and $(b-h-b_A)/t$ took the values, 20, 30, 40, 60 and 25, 35, 50, 75 respectively. Four panels, of varying lengths, were tested for each variant of panel geometry, so 256 panels were tested in all. Some of these were for values of h/b outside the range we are discussing; others had buckling stresses too great for accurate determination of the tangent modulus (required for calculation of f_o). For t_s/t = 1.00, 1.25 the cross-sectional area of the stringer flanges was large compared with that of the skin to which they were attached, and so the test specimens bore little relation to the theoretical model considered. However, there remains a large number of test results, and these are shown in Fig. 9.

Again, the scatter is noticeable. But the experimental points for t_s/t = 0.39 agree remarkably well with the theoretical curve.
For t_s/t = 0.63, however, the tendency is for the experimental points to be some 15% higher than the theoretical, while maintaining the general trend of variation. The reason for this is not yet understood.

REFERENCES

(1) Hickman, W.A., and Dow, N.F. — Compressive strength of 24 S - T aluminium-alloy flat panels with longitudinal formed hot-section stiffeners having four ratios of stiffener thickness to skin thickness. N.A.C.A. Technical Note 1553, March 1948.

(2) HU, P.C., Lundquist, E.E. and Batdorf, S.B. — Effect of small deviations from flatness on effective width and buckling of plates in compression N.A.C.A. Technical Note 1124, January 1947.

APPENDIX

The Effect of Initial Irregularities on the Estimation of Buckling Stress

For the special case of panels with simply supported edges, it is possible to allow for the effect of initial waving in the following manner. Assume a wave of amplitude H_o, and of the same wavelength as the final buckle system, to be present in the plate initially. The theoretical relations between $f_{average}$ (the average compressive stress carried by the plate) and f_{edge} (the compressive stress at the edge of the plate), and between f_{edge} and H (the amplitude of the "true" buckle), can then be calculated for a series of values of H_o/t; using approximate methods and large deflection plate theory. The results of such a calculation are shown in Figs. 10,11.

Thus, for three values of H/t;-

H_o/t	0.05	0.10	0.20
Drop in the initial value of Young's Modulus	2½%	3%	5%
Drop in f_b (f_a-f_e method)	3½%	7%	11-15%
Drop in f_b (H^2-f_e method)	1-2½%(?)	1-3%(?)	1-5%(?)

It will be seen that the $(\text{amplitude})^2$ - strain method of estimating buckling stress is less susceptible to error due to initial irregularities than is the load-strain method. However, as the $(\text{amplitude})^2$ - strain curve departs from the straight-line form, in the neighbourhood of $f_e/f_b = 1$, even with small H_o/t, it is impossible to use this method when failure follows closely after buckling.

As these results apply only to initial buckles having the same wavelength as the final system, they are of little use in correcting experimental observations for these effects. However, they do show how underestimates of f_b can arise in experimental work, and underline the need for the greatest possible accuracy in the manufacture of test panels used for the checking of theoretical work.

T A B L E I

b/h	20		10		8		7		6		5		4		3	
t_s/t	f_b/f_o	b/λ	f_b/f_o	b/λ	f_b/f_o	b/λ	f_b/f_o	b/λ	f_b/f_o	b/λ	f_b/f_o	b/λ	f_b/f_o	b/λ	f_b/f_o	b/λ
4/3	1.89	1.6	2.05	1.65	2.16	1.65	2.25	1.7	2.35	1.8	2.53	1.8	2.84	1.9	3.49	2.1
1	1.86	1.55	1.99	1.6	2.09	1.65	2.16	1.7	2.26	1.7	2.40	1.8	2.68	1.85	3.26	2.1
2/3	1.80	1.55			1.99	1.60					2.26	1.7			3.01	1.9
1/2															2.61	3.35
1/3	1.78	1.55			1.92	1.55					2.18	1.65	2.40	1.8	1.17	3.35
"0"	1.77	1.55	1.85	1.55	1.91	1.55	1.96	1.6	2.04	1.6	2.16	1.65	2.39	1.7	2.93	1.95

The row t_s/t = "0" is the solution of $F'^{n}(1) + (n-1)F^{n}_{n-1(1)} = 0$

THE BUCKLING STRESS IN COMPRESSION OF PANELS WITH SQUARE TOP-HAT SECTION STRINGERS

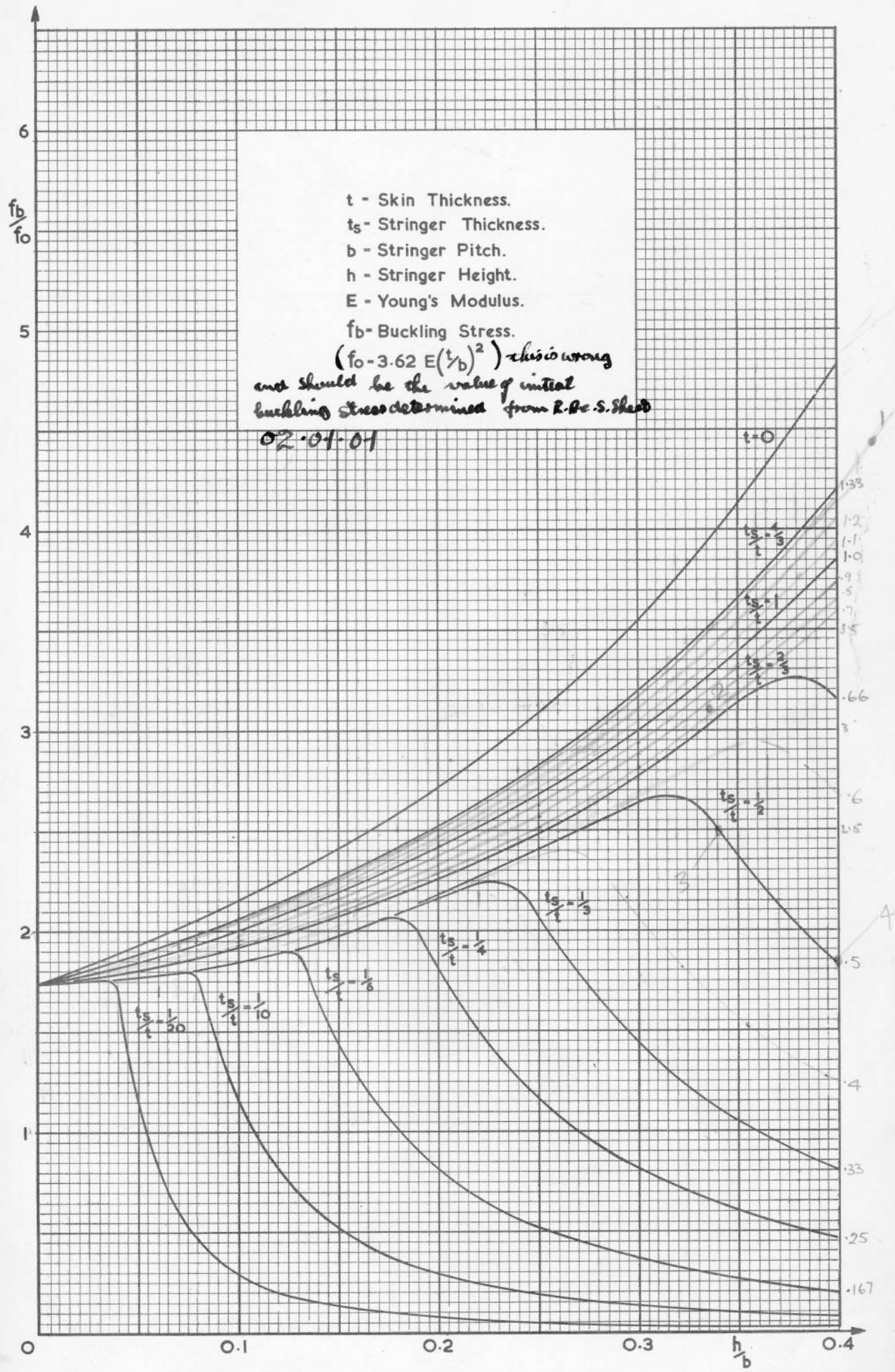

FIG. 7

C OF A.
REP. No.
29

+ Indicates estimations by Load strain method

× ---------- Amplitude^2-strain method

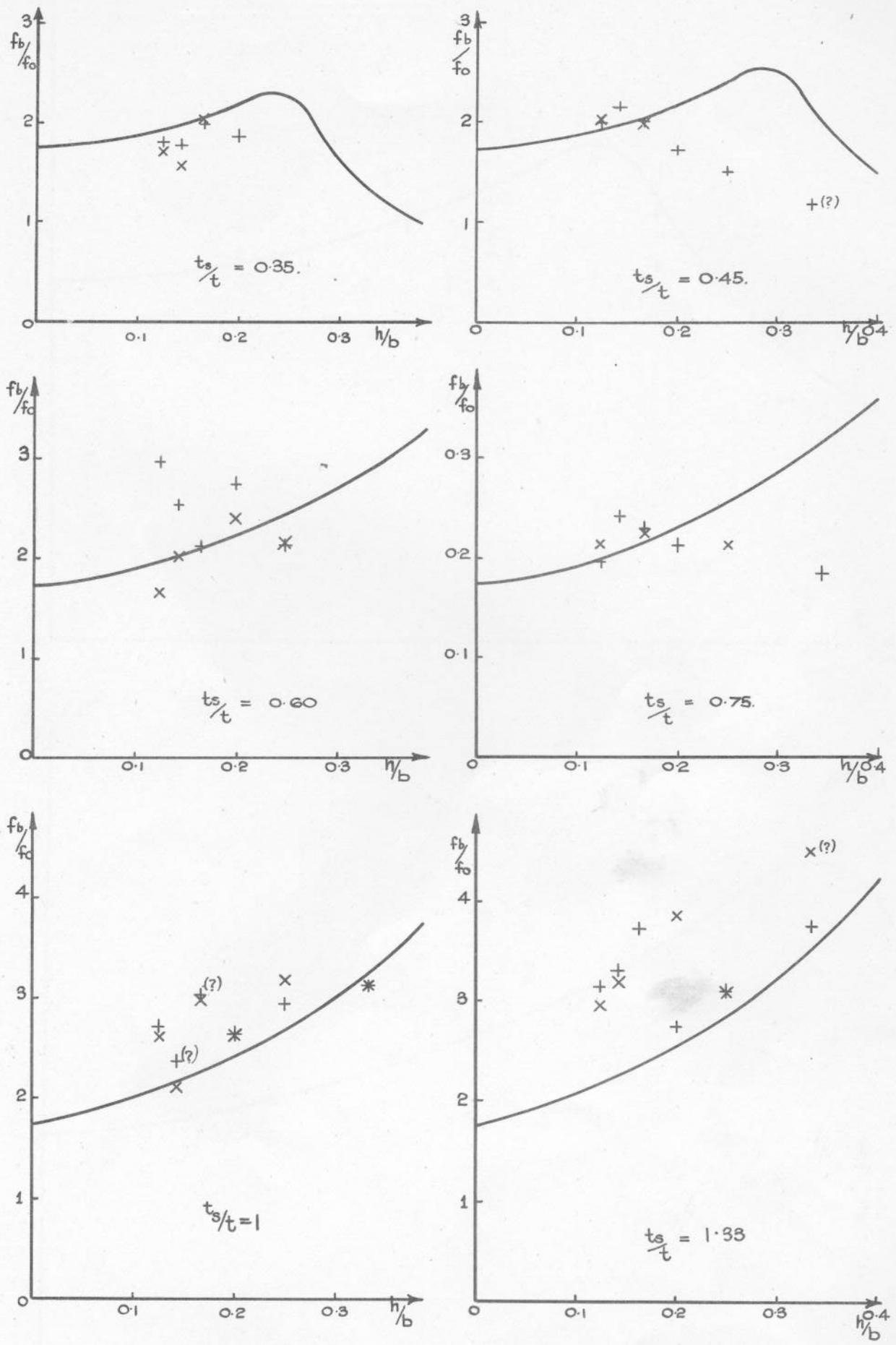

COMPARISON OF THE THEORETICAL RESULTS OF FIG. 7 WITH THE EXPERIMENTAL RESULTS OBTAINED BY A. J. MONK

FIG. 8

COMPARISON WITH AMERICAN RESULTS (NACA T.N.1553)

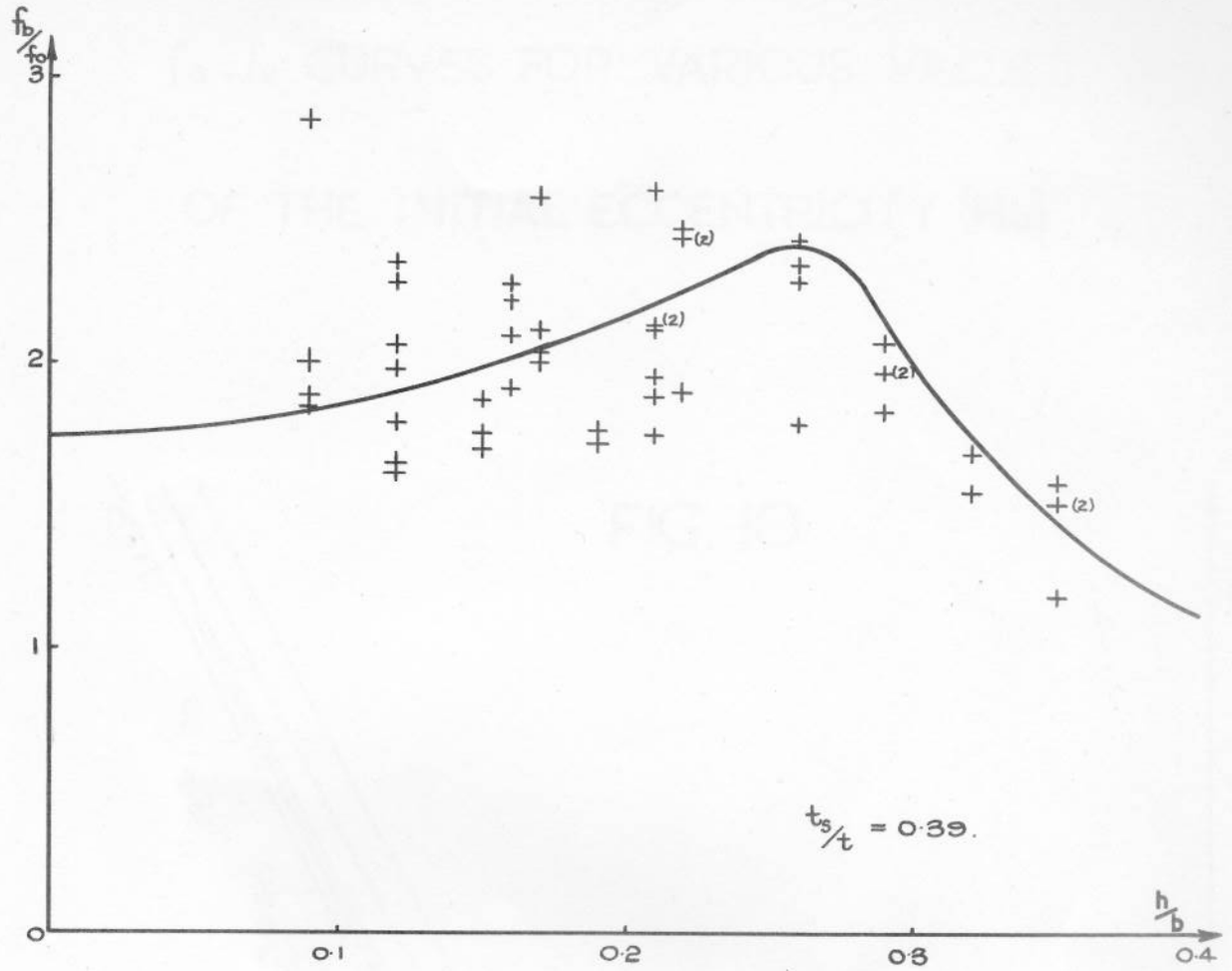

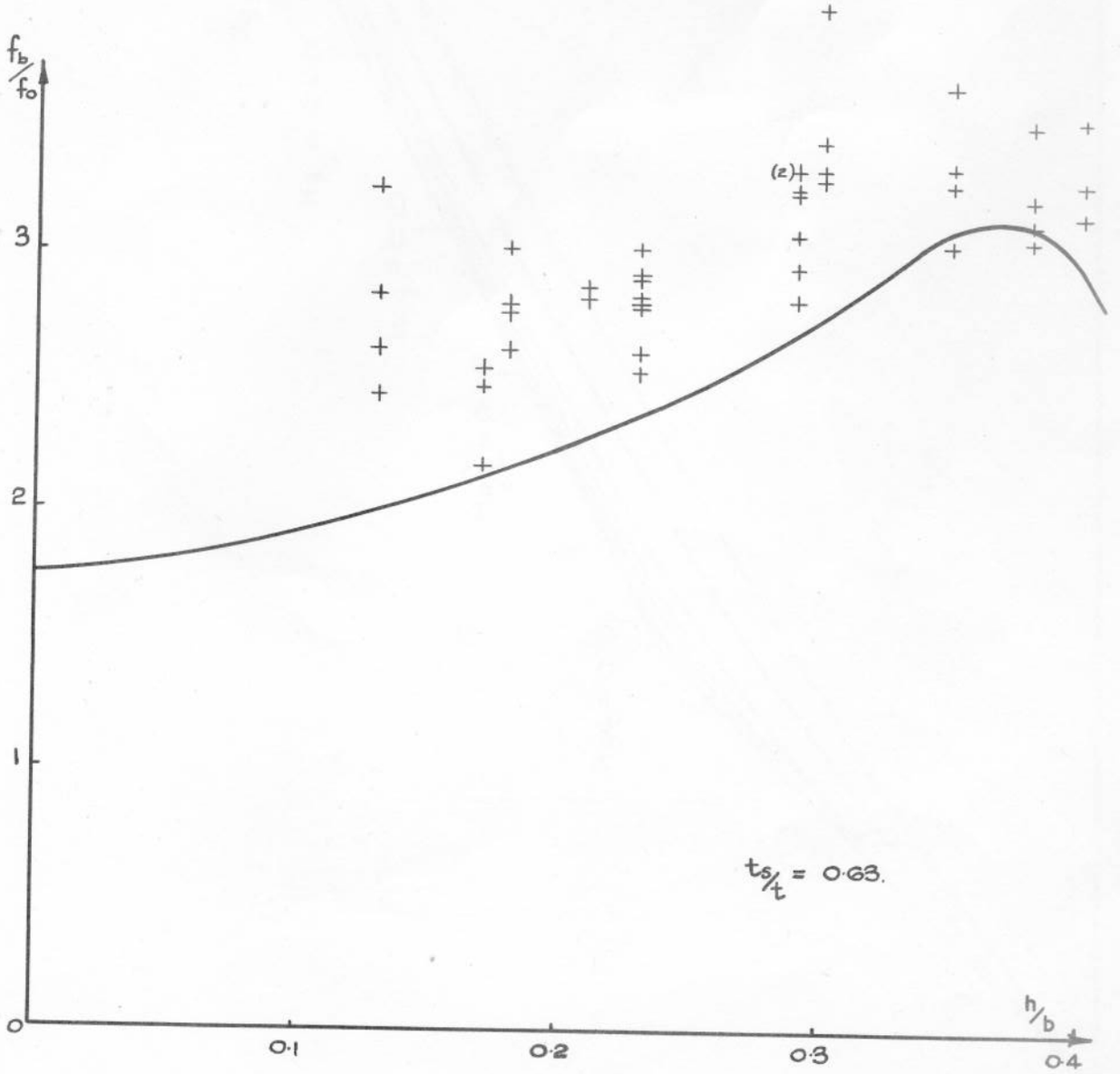

FIG. 9

$f_a - f_e$ CURVES FOR VARIOUS VALUES OF THE INITIAL ECCENTRICITY (H_o)

FIG. 10

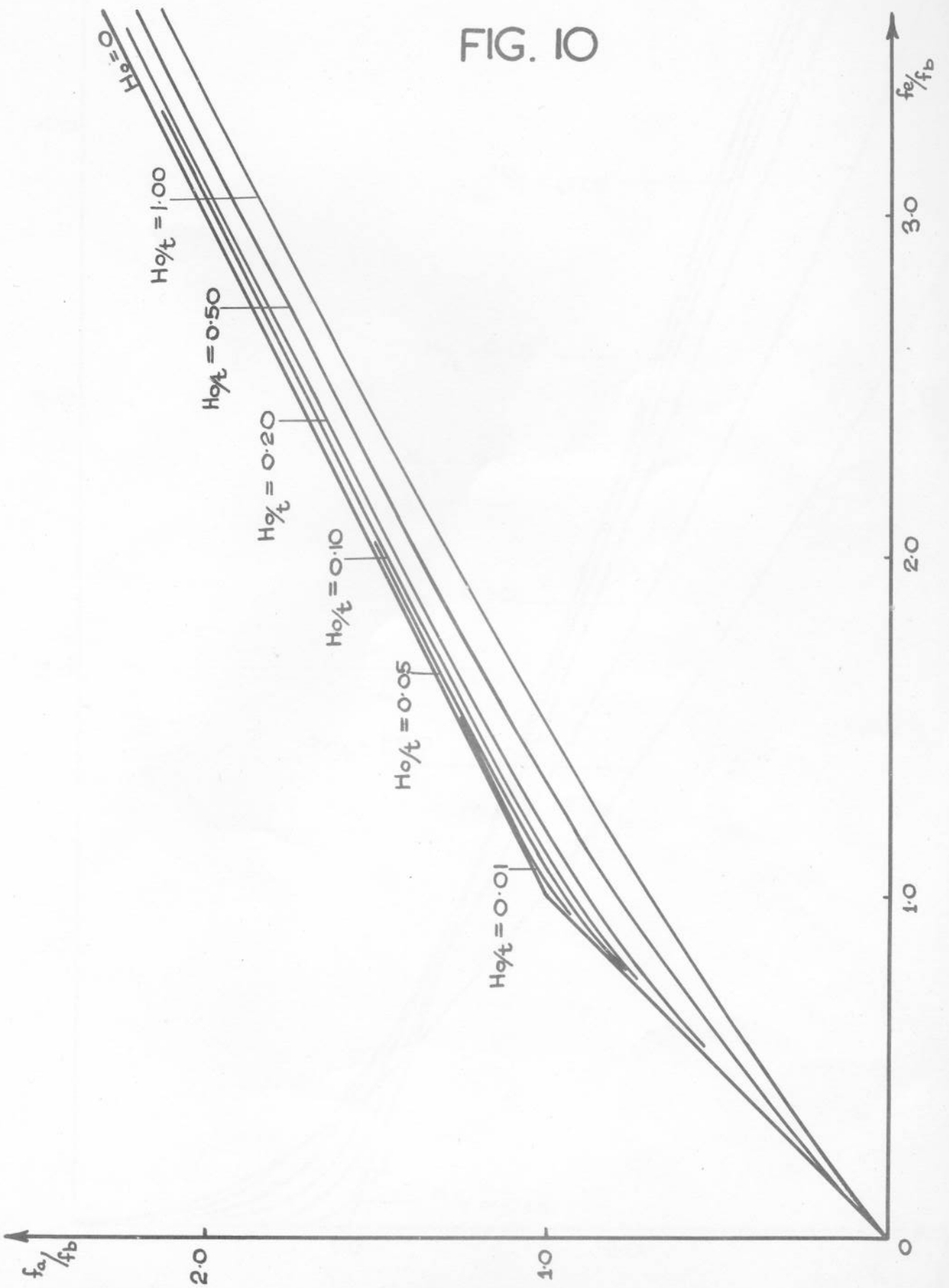

H^2 - f_e CURVES FOR VARIOUS H_o

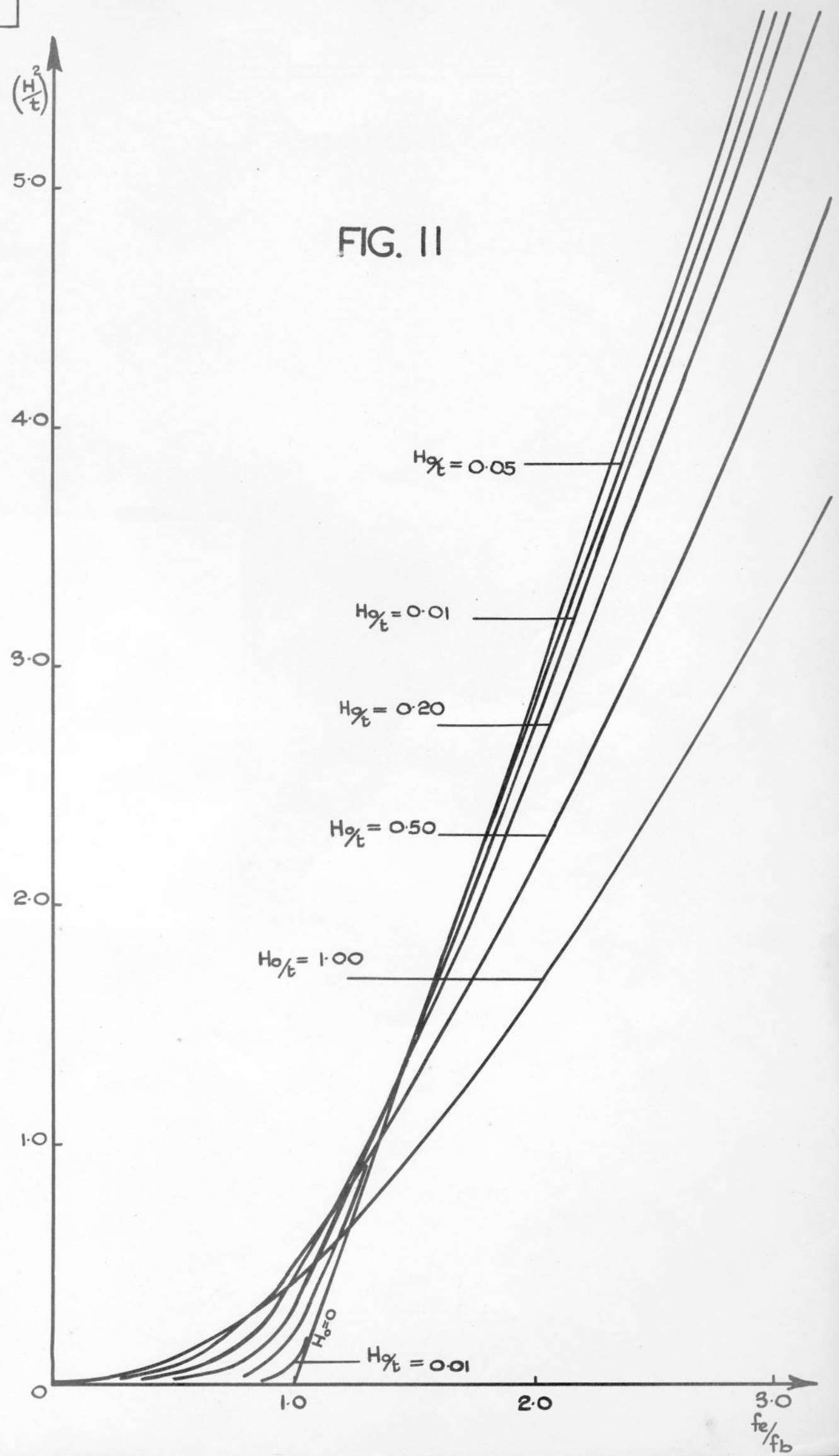

FIG. 11